Behavioral/Cognitive

Engagement of the GABA to KCC2 Signaling Pathway Contributes to the Analgesic Effects of A_3AR Agonists in Neuropathic Pain

Amanda Ford,[1] Annie Castonguay,[2,3] Martin Cottet,[2,3] Joshua W. Little,[4] Zhoumou Chen,[1] Ashley M. Symons-Liguori,[5] Timothy Doyle,[1] Terrance M. Egan,[1] Todd W. Vanderah,[5] Yves De Koninck,[2,3] Dilip K. Tosh,[6] Kenneth A. Jacobson,[6] and Daniela Salvemini[1]

[1]Department of Pharmacological and Physiological Science, St. Louis University School of Medicine, St. Louis, Missouri 63104, [2]Institut Universitaire en Santé Mentale de Québec, Québec City, Quebec G1J 2G3, Canada, [3]Department of Psychiatry & Neuroscience, Université Laval, Québec City, Quebec G1K 7P4, Canada, [4]Department of Surgery, Center for Anatomical Science and Education, St. Louis University School of Medicine, St. Louis, Missouri 63104, [5]Department of Pharmacology, College of Medicine, University of Arizona, Tucson, Arizona 85724-5050, and [6]Molecular Recognition Section, Laboratory of Bioorganic Chemistry, National Institute of Diabetes and Digestive and Kidney Diseases, National Institutes of Health, Bethesda, Maryland 20892-0810

More than 1.5 billion people worldwide suffer from chronic pain, yet current treatment strategies often lack efficacy or have deleterious side effects in patients. Adenosine is an inhibitory neuromodulator that was previously thought to mediate antinociception through the A_1 and A_{2A} receptor subtypes. We have since demonstrated that A_3AR agonists have potent analgesic actions in preclinical rodent models of neuropathic pain and that A_3AR analgesia is independent of adenosine A_1 or A_{2A} unwanted effects. Herein, we explored the contribution of the GABA inhibitory system to A_3AR-mediated analgesia using well-characterized mouse and rat models of chronic constriction injury (CCI)-induced neuropathic pain. The deregulation of GABA signaling in pathophysiological pain states is well established: GABA signaling can be hampered by a reduction in extracellular GABA synthesis by GAD65 and enhanced extracellular GABA reuptake via the GABA transporter, GAT-1. In neuropathic pain, $GABA_A$R-mediated signaling can be further disrupted by the loss of the KCC2 chloride anion gradient. Here, we demonstrate that A_3AR agonists (IB-MECA and MRS5698) reverse neuropathic pain via a spinal mechanism of action that modulates GABA activity. Spinal administration of the $GABA_A$ antagonist, bicuculline, disrupted A_3AR-mediated analgesia. Furthermore, A_3AR-mediated analgesia was associated with reductions in CCI-related GAD65 and GAT-1 serine dephosphorylation as well as an enhancement of KCC2 serine phosphorylation and activity. Our results suggest that A_3AR-mediated reversal of neuropathic pain increases modulation of GABA inhibitory neurotransmission both directly and indirectly through protection of KCC2 function, underscoring the unique utility of A_3AR agonists in chronic pain.

Key words: **adenosine; adenosine receptors; GABA; KCC2; neuropathic pain**

Introduction

Chronic pain represents an enormous socioeconomic public health problem that severely limits quality of life for its sufferers. Unfortunately, current treatment strategies are either ineffective (Dworkin et al., 2007) or are accompanied by unacceptable side effects (McNicol et al., 2003).

Received Oct. 29, 2014; revised Feb. 27, 2015; accepted March 5, 2015.

Author contributions: A.F. and D.S. designed research; A.F., A.C., M.C., J.W.L., Z.C., T.D., and T.M.E. performed research; T.W.V., Y.D.K., D.K.T., and K.A.J. contributed unpublished reagents/analytic tools; A.F., A.C., M.C., J.W.L., A.M.S.-L., T.D., T.M.E., and D.S. analyzed data; A.F., A.C., J.W.L., A.M.S.-L., T.D., T.W.V., Y.D.K., and D.S. wrote the paper.

This study was supported by National Cancer Institute Grant R01CA169519, the St. Louis Cancer Center, the Canadian Institutes of Health Research (MOP 12942), and the National Institute of Diabetes and Digestive and Kidney Diseases Intramural Research Program. We thank Joe Henry Steinbach (Washington University, St. Louis) for the gift of plasmids encoding the GABA subunits.

We declare no competing financial interests.

Correspondence should be addressed to Dr. Daniela Salvemini, Department of Pharmacological and Physiological Science, St. Louis University School of Medicine, 1402 S. Grand Blvd, St. Louis, MO 63104. E-mail: salvemd@slu.edu.

DOI:10.1523/JNEUROSCI.4495-14.2015

 0270-6474/15/356057-11$15.00/0

Adenosine, an endogenous purine nucleoside whose actions are mediated through the activation of four G-protein-coupled adenosine receptor (AR) subtypes (A_1, A_{2A}, A_{2B}, and A_3), has been hypothesized to play an inhibitory role in nociceptive pathways. Indeed, adenosine and selective AR agonists have potent antinociceptive effects in neuropathic pain of various etiologies (Sawynok, 2007). However, the clinical use of A_1/A_2AR agonists is limited by serious cardiovascular side effects (Zylka, 2011). We recently demonstrated that A_3AR agonists have potent analgesic actions in several models of chronic neuropathic pain (Chen et al., 2012; Janes et al., 2014, 2015; Little et al., 2015). Interestingly, selective, orally bioavailable A_3AR agonists, such as 1-deoxy-1-[6-[[(3-iodophenyl)methyl]amino]-9*H*-purin-9-yl]-*N*-methyl-β-D-ribofuranuronamide (IB-MECA), are in Phase II/III clinical trials for non–pain-related indications and exhibit acceptable safety profiles (Fishman et al., 2012).

Although evidence supports the use of A_3AR agonists in the management of chronic pain, the underlying mechanism(s) of action are unknown. A_3ARs are expressed throughout the nervous system in relevant pain areas (i.e., the rostral ventromedial

medulla and the dorsal horn of the spinal cord) and found in neurons and glial cells (Borea et al., 2015; Little et al., 2015). We have characterized the central effects of A_3AR, finding that A_3AR activation inhibits nociception by engaging bulbospinal analgesic pathways and suppressing the responses of spinal wide dynamic range projection neurons during persistent pain states (Little et al., 2015). Despite the potent inhibitory actions of A_3AR on neurotransmission, A_3AR analgesia is not mediated by opioid or endocannabinoid pathways (Chen et al., 2012; Little et al., 2015). We therefore questioned whether A_3AR agonists might exert their inhibitory actions on nociception by engaging the GABA inhibitory system.

In neuropathic pain states, tonic GABA inhibition is suppressed in superficial dorsal horn nociceptive neurons and enhanced excitatory signaling is no longer regulated by inhibitory controls, leading to a net neuronal hyperexcitability (Zeilhofer et al., 2012). Loss of GABA inhibition can result from a number of pathophysiological changes in key components throughout the GABA system. In pathophysiological pain states, reduced levels of spinal GABA (Stiller et al., 1996; Eaton et al., 1998) and its synthesizing enzyme, GAD65 (Eaton et al., 1998; Moore et al., 2002) are observed, whereas the functional expression of the GABA transporter GAT-1, which removes GABA from the synapse (Daemen et al., 2008; Liu et al., 2013), is increased. Additionally, there is a reduction in the activity and expression of the K^+-Cl^- cotransporter, KCC2 (Coull et al., 2003; Price et al., 2005), which maintains the anion gradient necessary for the inhibitory actions of the $GABA_A$ receptor ($GABA_AR$) in neurons. This impairment of GABA signaling produces behavioral hypersensitivity resembling that observed after peripheral nerve injury (Enna and McCarson, 2006). While therapies that enhance GABAergic signaling produce significant analgesia (Malan et al., 2002; McCarson and Enna, 2014), the use of pro-GABAergic therapies as analgesics remains limited by adverse CNS side effects.

Taken together, we hypothesize that A_3AR agonists reverse neuropathic pain by modulating key components that regulate chloride-mediated inhibition at the spinal level.

Materials and Methods

Experimental animals. Male Sprague Dawley rats (200–220 g starting weight) or male CD1 mice (20–30 g) from Harlan Laboratories were housed 2–4 per cage (for rats) and 5 per cage (for mice) in a controlled environment (12 h light/dark cycle) with food and water available *ad libitum*. All experiments were performed in accordance with the International Association for the Study of Pain and the National Institutes of Health guidelines on laboratory animal welfare and the recommendations by St. Louis University Institutional Animal Care and Use Committee. All experiments were conducted with the experimenters blinded to treatment conditions.

Chronic constriction injury (CCI) model. CCI to the sciatic nerve of the left hind leg in mice and rats was performed under general anesthesia using the well-characterized Bennett model (Bennett and Xie, 1988). Briefly, animals were anesthetized with 3% isoflurane/O_2 inhalation and maintained on 2% isoflurane/O_2 for the duration of surgery. The left thigh was shaved, scrubbed with Nolvasan, and a small incision (1–1.5 cm in length) was made in the middle of the lateral aspect of the left thigh to expose the sciatic nerve. The nerve was loosely ligated around the entire diameter of the nerve at three distinct sites (spaced 1 mm apart) using silk sutures (6.0, mice; 4.0, rats). The surgical site was closed with a single muscle suture and a skin clip. Pilot studies established that under our experimental conditions peak mechano-allodynia develops by D7-D10 following CCI. Test substances or their vehicles were given intraperitoneally (i.p.) at peak mechano-allodynia.

Test compounds. IB-MECA was purchased from Tocris Bioscience. MRS1523 (3-propyl-6-ethyl-5-[(ethylthio)carbonyl]-2-phenyl-4-propyl-3-pyridine-carboxylate), bicuculline ([R-(*R**,*S**)]-6-(5,6,7,8-tetrahydro-6-methyl-1,3-dioxolo[4,5-*g*]isoquinolin-5-yl)furo[3,4-*e*]-1,3-benzodioxol-8(6*H*)-one), and VU0240551 (*N*-(4-methyl-2-thiazolyl)-2-[(6-phenyl-3-pyridazinyl)thio]-acetamide) were obtained from Sigma-Aldrich. MRS5698 ((1*S*,2*R*,3*S*,4*R*,5*S*)-4-(6-((3-chlorobenzyl)amino)-2-((3,4-difluorophenyl) ethynyl)-9*H*-purin-9-yl)-2,3-dihydroxy-*N*-methylbicyclo[3.1.0]hexane-1-carboxamide) was synthesized as previously described (Tosh et al., 2012).

Behavioral testing. Mechano-allodynia was measured after animals were allowed to acclimate to elevated cages with a wire mesh floor for 15 min. The plantar aspect of the hindpaw was probed with calibrated von Frey filaments (Stoelting; mice: 0.07–2.00 g; rats: 0.407–26 g) according to the "up-and-down" method (Dixon, 1980) (see Fig. 2). Behavioral testing was done before surgery on D0, on D7 after surgery (peak development of mechano-allodynia), and at different time points (30 min to 5 h) after drug/vehicle administration (given on D7). Animals were then killed by asphyxiation with CO_2 and subsequently decapitated as a secondary method, and tissues were collected for further examination.

Electrophysiology. Cultured HEK293 cells were transfected with equal amounts (1 μg) of cDNA encoding the a_1, b_2, and γ_{2L} subunits of the rat $GABA_A$ receptor and eGFP (0.3 μg) using Effectene (QIAGEN). Agonist-induced changes in membrane current were recorded using the amphotericin perforated-patch technique as previously described (Samways et al., 2011). Drugs were applied by using the Perfusion Fast-Step SF-77 System (Warner Instruments).

Immunoblotting. Dorsal horn tissues were obtained from the lower lumbar enlargement (L4-L6) region of the spinal cord and stored immediately at −80°C. Relative protein expression was assessed as previously described (Doyle et al., 2011). Briefly, frozen tissues were homogenized in lysis buffer [20 mM Tris-Cl, pH 7.4, 150 mM NaCl, 0.1% CHAPS, 0.5% Triton X-100, 0.1% SDS, 2 mM EGTA, 5% glycerol, 50 mM sodium fluoride, 1 mM sodium orthovanadate, 1 mM sodium molybdinate, 0.1 M PMSF, 1× phosphatase inhibitor mixture (Sigma-Aldrich), and 1× protease inhibitor mixture (Sigma-Aldrich)], sonicated, and clarified by centrifugation. Total protein concentration was determined by BCA, and samples were heat denatured in 2× Laemmli buffer supplemented with β-mercaptoethanol and then stored at −20°C until assayed. Proteins were resolved by Tris-glycine-SDS electrophoresis with a 4%–20% gel and transferred to nitrocellulose membrane (Bio-Rad). After blocking with 5% nonfat milk or 5% BSA in PBS-T, the membranes were probed overnight at 4°C with primary antibody. Bands were visualized with secondary HRP-conjugated anti-rabbit IgG antibodies (Cell Signaling Technology, 1:2500). Immunoblot images were captured and analyzed using ChemiDoc MP and Image Lab 5.0 (Bio-Rad). All data are expressed as the percentage densitometric signal from the ipsilateral lysate over the animal-matched contralateral lysate normalized to respective β-actin loading control.

Immunoprecipitation. Total serine phosphorylated protein fractions were immunoprecipitated from ipsilateral and contralateral spinal cord lysates (250 μg). Briefly, agarose-conjugated mouse monoclonal anti-phosphoserine beads (Sigma) were equilibrated in immunoprecipitation buffer (20 mM Tris-Cl, pH 7.4, 150 mM NaCl, 1 mM EDTA, 1 mM EGTA, 10% glycerol) supplemented with 1 mM PMSF, 50 mM NaF, 1 mM Na_3VO_4, 1 mM Na_3MbO_4, and 1× phosphatase and protease inhibitor mixtures (Sigma). The equilibrated beads (25 μl) were added to each total protein lysate (250 μg) and brought to 500 μl with immunoprecipitation buffer. After incubation for 18 h at 4°C with continuous inversion, the lysates/bead mixtures were centrifuged 5 min at 1000 × *g* at 4°C and the supernatant was collected for β-actin (Sigma, 1:2000) analysis of protein loading. The beads were washed 3 times with ice-cold 1× PBS with centrifugation for 5 min at 1000 × *g* at 4°C then heat-denatured in 2× Laemmli buffer (25 μl) supplemented with β-mercaptoethanol for 5 min at 95°C. The denatured supernatant was subjected to SDS-PAGE (4%–20% TGX, Bio-Rad) and immunoblotting to nitrocellulose. The serine phosphorylation of KCC2, GAT1, and GAD65 was identified by enhanced chemiluminescence using antibodies to KCC2 (Millipore, 1:1000); GAT1 (Abcam, 1:1000), GAD65 (Cell Signaling Technology, 1:1000), and secondary HRP conjugated anti-rabbit IgG antibodies (Cell Signaling Technology, 1:2500). Immunoblot images were captured and

analyzed using ChemiDoc MP and Image Lab 5.0 (Bio-Rad). All data are expressed as the percentage densitometric signal from the ipsilateral lysate over the animal-matched contralateral lysate normalized to respective β-actin loading control.

Immunofluorescence. After behavioral measurements, lumbar spinal cords were harvested from rats, placed into cryomolds containing optimal cutting temperature embedding compound (Electron Microscopy Sciences), rapidly frozen in an isopropanol/dry ice bath, and stored at −80°C. Transverse sections (20 μm) were cut in a cryostat, collected on gelatin-coated glass microscope slides, and stored at −20°C. Spinal cord sections were fixed in 10% buffered neutral formalin (10 min), rinsed in PBS, blocked for 1 h (10% normal goat serum, 2% BSA, 0.2% Triton X-100 in PBS), and then immunolabeled as previously described (Little et al., 2012) using a primary antibody, rabbit IgG polyclonal anti-KCC2 phosphorylated serine 940 (pKCC2; 1:100, incubated 18 h at 4°C, Rockland), followed by several PBS rinses and incubation (2 h room temperature in the dark) with a goat anti-rabbit IgG antibody conjugated to AlexaFluor-568 (1:250, Invitrogen). After a series of PBS rinses, coverslips were mounted with Fluorogel II containing DAPI (Electron Microscopy Sciences) and photographed with an Olympus FV1000 MPE confocal microscope (multiline argon lasers with excitation at 405 and 543 nm) using a 10× objective (UPLSAPO; 0.4 NA) for regional fluorescence intensity image analysis and a 20× objective (UPLSAPO; 0.75 NA) and 60× oil-immersion objective (PLAPON; 1.42 NA) with 2.4× optical zoom (0.1 μm pixel dimensions in the *x-y* plane and the pinhole set at 1 Airy unit) for higher-magnification images. Images were acquired within the dynamic range of the microscope (i.e., no pixel intensity values of 0 or 255 in an 8-bit image). Sections omitting primary antibody or treated with rabbit IgG at equivalent concentrations to primary antibodies were used as controls yielding only nonspecific background fluorescence. The fluorescence intensity of immunolabeled pKCC2 was calculated as previously reported (Little et al., 2012) in the superficial dorsal horn (laminae I and II) of the lumbar spinal cord. The mean fluorescence intensity (MFI) was calculated by Equation 1 as follows:

$$\mathrm{MFI} = \mathrm{i}(\mathrm{pp}^2 \div \mathrm{p}^2) \quad (1)$$

where i is the mean gray value, pp is the positive pixel area, and p is total pixel area. Image analysis was performed using the NIH freeware program ImageJ (version 1.43) (Rasband, 1997–2011). Images received background threshold corrections before analysis using the automated ImageJ intermodes histogram-based threshold function. The superficial dorsal horn was outlined on images at the L4, L5, and L6 levels bilaterally using the ImageJ ROI tool. The borders of this region were determined and confirmed using cresyl violet-stained sections of regions adjacent to immunolabeled sections and an atlas (Paxinos and Watson, 1998). Relative MFI was calculated as fold change normalized to the fluorescence intensity of the contralateral (unaffected) dorsal horn (i.e., dividing the fluorescence intensity from superficial dorsal horn of the ipsilateral side by the contralateral side). Data are expressed as arbitrary units.

Imaging of Cl^- transport in rat spinal cord neurons. Parasagittal spinal slices (400 μm thick) were prepared from rats using a Leica VT1200S Vibratome as previously described (Chéry et al., 2000). Briefly, rats were anesthetized and perfused with ice-cold sucrose ACSF (sACSF), and the spinal cord was retrieved by hydraulic extrusion. After slicing, sections were kept in bubbled ACSF at 34°C. For CCI and sham rats, imaging was only performed on slices ipsilateral to the nerve injury. The paw withdrawal threshold was assessed on each animal before slicing and also 1 h after intraperitoneal injection of MRS5698, to confirm the reversal of allodynia (score >4 g).

KCC2-dependent Cl^- transport rate was imaged as previously described (Ferrini et al., 2013). Intracellular Cl^- slices were incubated in ACSF containing 5 mM the Cl^- indicator MQAE (*N*-(ethoxycarbonylmethyl)-6-methoxyquinolinium bromide, Invitrogen) for 30–40 min and then transferred to a perfusion chamber (2 ml/min) to wash out extracellular MQAE for 10 min. To minimize KCC2-independent Cl^- transport, the ACSF used for imaging contained 1 μM TTX, 10 μM CNQX, 40 μM AP5, 1 μM strychnine, and 10 μM gabazine. Fluorescence lifetime imaging of MQAE was acquired as previously described (Doyon et al., 2011; Ferrini et al., 2013). Instrument response function of the detection path was acquired using an 80 nm gold nanoparticle suspension to generate second-harmonic signal. Recorded cells were visually identified by merging transmitted light and MQAE fluorescence. Lifetime images were acquired every 10 s for a period of 7 min. After a control period of 50 s, perfusion solution was switched to ACSF containing 15 mM KCl (osmolarity adjusted using mannitol) to reverse KCC2-mediated Cl^- transport (Chorin et al., 2011). Lifetime measurements were compiled over time after the switch in extracellular $[K^+]$ to quantify the rate of Cl^- import in cells through KCC2. Lifetime values for each cell were averaged over the whole-cell body area and extracted for each time point using custom MATLAB software. Briefly (Digman et al., 2008), we converted the photon timing histograms of each acquired lifetime image to phasor plots. Then, for every time-point, ROIs corresponding to cell bodies were selected and added to a new phasor. Lifetimes of all cells bodies were averaged for each slice at each time point to generate the lifetime time course. All transport rates were tested with the same starting $[Cl^-]_i$ (i.e., in the period when there is no Cl^- load prior to the change in extracellular K^+).

ED_{50} calculations. The ED_{50} for the A_3AR agonists, IB-MECA and MRS5698, to reverse mechano-allodynia from CCI was determined by a three-parameter, nonlinear regression analysis of normalized paw withdrawal threshold (PWT) data using the following equation:

$$\%\mathrm{Reversal} = (\mathrm{PWT}_{1\mathrm{h}} - \mathrm{PWT}_{\mathrm{D7}})/(\mathrm{PWT}_{\mathrm{DO}} - \mathrm{PWT}_{\mathrm{D7}}) \times 100$$

where $\mathrm{PWT}_{1\,\mathrm{h}}$ = PWT (g) at 1 h after agonist injection on D7, $\mathrm{PWT}_{\mathrm{D7}}$ = PWT (g) on D7 before agonist, and $\mathrm{PWT}_{\mathrm{D0}}$ = PWT (g) on D0 before surgery. Nonlinear regression analysis was performed using GraphPad Prism version 5.04 (GraphPad Software).

Statistical analysis of data. Data are expressed as mean ± SEM for *n* animals. Time-dependent behavior was analyzed by two-tailed, two-way repeated-measures ANOVA with Bonferroni *post hoc* comparisons to D7 behaviors. Data for Cl^- transport were analyzed by one-way ANOVA followed by Bonferroni *post hoc* comparisons. Protein expression data were determined by Welch's corrected, unpaired, one-tailed, Student's *t* test. Significant differences were defined as a value of $p < 0.05$. All statistical analysis was performed using SPSS (Release 21.0, IBM).

Results

A_3AR agonists reverse CCI-induced mechano-allodynia via a spinal site of action

To examine a potential site of action for the anti-allodynic effects of A_3AR agonists, mice were pretreated intrathecally with the selective A_3AR antagonist MRS1523 (Li et al., 1998) prior to the systemic administration of IB-MECA. As previously demonstrated (Chen et al., 2012), systemic IB-MECA (1.0 mg/kg; i.p.; $n = 6$) given on D7 significantly reverses established mechano-allodynia in the CCI model with peak reversal occurring at 1 h. Local blockade of spinal A_3AR with MRS1523 (3 nmol; $n = 6$), given by intrathecal (i.th.) injection completely blocked IB-MECA's anti-allodynic effects (Fig. 1*A*; repeated-measures ANOVA, $F_{(2,4)} = 75.4$, $p = 0.001$), whereas MRS1523 alone had no effect.

To confirm that IB-MECA exerts antinociception at the level of the spinal cord, we examined the antinociceptive properties of IB-MECA when administered spinally. As expected, intrathecal administration of IB-MECA (3, 10, 30, or 60 nmol; i.th.; $n = 6$), but not its vehicle, dose-dependently reversed CCI-induced mechano-allodynia with a peak reversal at 1 h and an ED_{50} of 7.73 nmol (95% CI: 5.2–11.5; Fig. 1*B*; Greenhouse–Geisser corrected repeated-measures ANOVA, $\varepsilon = 0.474$, $F_{(6,24)} = 12.1$, $p = 0.001$).

To extend our previous work and strengthen evidence of a role for A_3AR agonism in pain relief, we used the agent MRS5698, which represents a chemical class unique from IB-MECA. MRS5698 is both orally bioavailable and >1000-fold more selective for A_3AR over other AR subtypes; as such, MRS5698 is an

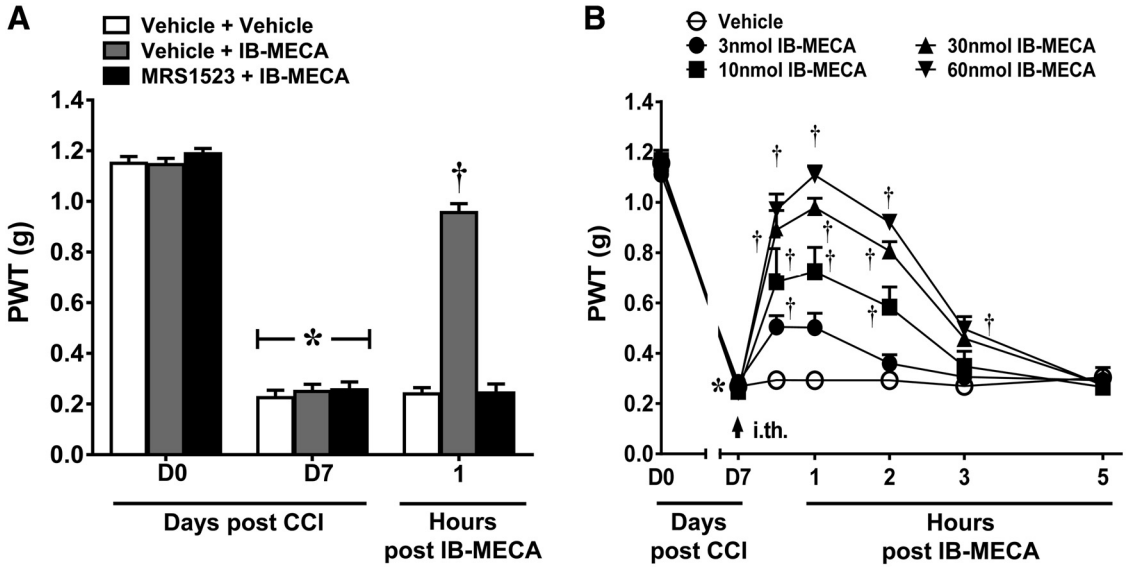

Figure 1. IB-MECA's beneficial actions involve a central mechanism of action. Compared with D0, CCI led to a time-dependent development of mechano-allodynia by D7 that was reversed by IB-MECA (1.0 mg/kg; i.p.), but not its vehicle (***A***, ***B***). ***A***, Pretreatment with intrathecal MRS1523 (3 nmol) prevented the beneficial effects. ***B***, Intrathecal administration of IB-MECA (arrow) dose-dependently reversed CCI-induced mechano-allodynia. Data are mean ± SEM; $n = 6–8$ mice. *$p < 0.05$ for D7 versus D0 (repeated-measures ANOVA with Bonferroni *post hoc* comparisons to D7). †$p < 0.05$ for t_h post-IB-MECA versus D7 (repeated-measures ANOVA with Bonferroni *post hoc* comparisons).

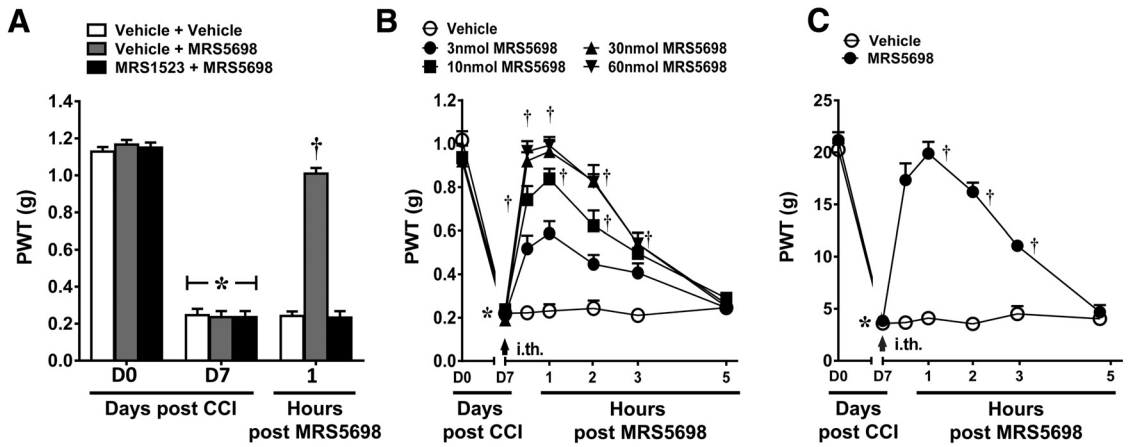

Figure 2. MRS5698 reverses CCI-induced mechano-allodynia via spinal mechanisms in both mouse and rat. In mice, CCI led to the time-dependent development of mechano-allodynia by D7 that was reversed by MRS5698 (1.0 mg/kg; i.p.), but not its vehicle. Pretreatment with intrathecal MRS1523 (3 nmol) prevented the anti-allodynic effects (***A***) in a dose-dependent manner (***B***). Intrathecal administration of MRS5698 (arrow) at the highest dose (60 nmol) also reversed mechano-allodynia in a rat model of CCI (***C***). Data are mean ± SEM; $n = 6$ mice or rats. *$p < 0.05$ for D7 versus D0 (repeated-measures ANOVA with Bonferroni comparisons). †$p < 0.05$ for t_h post-IB-MECA versus D7 (repeated-measures ANOVA with Bonferroni comparisons).

excellent pharmacological tool for investigating the mechanism(s) of A_3AR analgesia (Tosh et al., 2012). As with IB-MECA, systemic MRS5698 dose-dependently reverses CCI-induced mechano-allodynia (Little et al., 2015). Spinal MRS5698 (3, 10, 30, 60 nmol; i.th.; $n = 6$) dose-dependently reversed mechano-allodynia with a calculated ED_{50} of 6.2 nmol (95% CI: 4.1–9.4; Fig. 2*B*; Greenhouse–Geisser corrected repeated-measures ANOVA, $\varepsilon = 0.655$, $F_{(6,24)} = 15.9$, $p = 0.001$). Moreover, inhibiting spinal A_3AR signaling with intrathecal MRS1523 (3.0 nmol; $n = 6$) blocked the anti-allodynic effects of systemic MRS5698 (1.0 mg/kg; i.p.; $n = 6$), confirming an A_3AR mechanism of action at the spinal level (Fig. 2*A*; repeated-measures ANOVA, $F_{(2,4)} = 90.2$, $p = 0.001$). We extended our findings to another rodent model of CCI: as in the mouse model, spinal MRS5698 (60 nmol; i.th.; $n = 6$) reversed CCI-induced mechano-allodynia in rats (Fig. 2*C*; Greenhouse–Geisser corrected repeated-measures ANOVA, $\varepsilon = 0.242$, $F_{(6,6)} = 5.9$, $p = 0.019$), whereas the vehicle had no effect.

Bicuculline blocks the anti-allodynic actions of MRS5698

To assess whether the spinal mechanism(s) of action of A_3AR agonists might involve GABAergic signaling, we first tested whether the anti-allodynic actions of MRS5698 are dependent on spinal $GABA_A$ receptor activation. Spinal pretreatment with the selective $GABA_A$ antagonist, bicuculline (0.5 μg; i.th.; $n = 6$), 15 min before systemic MRS5698 (1.0 mg/kg; i.p.; $n = 6$) abolished the ability of MRS5698 to reverse CCI-induced mechano-allodynia. This effect was observed in both mouse (Fig. 3*A*; Greenhouse–Geisser corrected repeated-measures ANOVA, $\varepsilon = 0.297$, $F_{(6,12)} = 8.8$, $p = 0.001$) and rat models of CCI (Fig. 3*B*; Greenhouse–Geisser corrected repeated-measures ANOVA, $\varepsilon = 0.275$, $F_{(6,12)} = 8.4$, $p = 0.001$) with the dose chosen from previ-

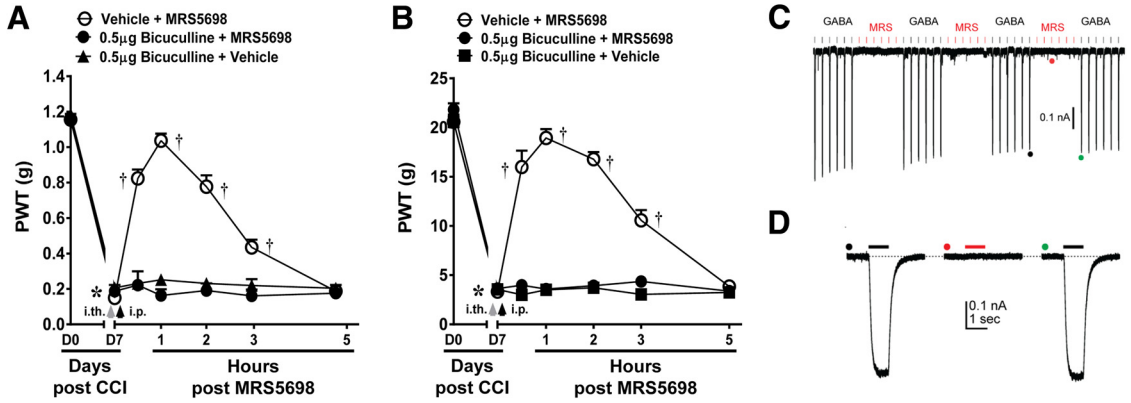

Figure 3. Bicuculline blocks the anti-allodynic actions of MRS5698. In both mouse (***A***) and rat (***B***) models, MRS5698 (gray arrow; 1.0 mg/kg; i.p.) led to a time-dependent development of mechano-allodynia, blocked by pretreatment with bicuculline (black arrow; 0.5 μg; i.th.). Bicuculline alone had no effect (***A***, ***B***). GABA (1 μM) evoked robust and reproducible inward currents in voltage-clamped ($V_{hold} = -60$ mV) HEK293 cells transiently expressing either rat a_1b_2 ($n = 5$) or $a_1b_2g_{2L}$ ($n = 5$) $GABA_A$ receptors. By contrast, MRS5698 (10 μM) had no effect (***C***). Traces marked with filled circles are shown at an expanded time-scale in ***D***. Data are mean ± SEM; $n = 6$. *$p < 0.05$ for D7 versus D0 (repeated-measures ANOVA with Bonferroni comparisons). †$p < 0.05$ for t_h post-IB-MECA versus D7 (repeated-measures ANOVA with Bonferroni comparisons).

ous literature (Nowak et al., 1982). At the dose tested, bicuculline did not affect PWT in naive animals (data not shown). Of note, we have determined that MRS5698 is not a $GABA_A$ agonist: interactions of MRS5698 with off-target receptor sites were measured for the most promising leads from *in vivo* screening. Off-target binding sites (mostly GPCRs) were assayed in a broad high-throughput screen of binding activity using cloned human or rodent cDNAs for CNS receptors and ion channels (in ~50 assays). This screening was provided by the National Institute of Mental Health Psychoactive Drug Screening Program. MRS5698 was tested at a concentration of 10 μM and did not show significant binding to $GABA_A$ receptors (Paoletta et al., 2014). The inability of MRS5698 to act as a $GABA_A$ receptor agonist was confirmed electrophysiologically using the perforated-patch technique. GABA (1 μM) evoked robust and reproducible inward currents in voltage-clamped HEK293 cells ($V_{hold} = -60$ mV) that transiently expressed either rat a_1b_2 ($n = 5$) or $a_1b_2g_{2L}$ ($n = 5$) $GABA_A$ receptors. In contrast, MRS5698 (10 μM) had no effect (Fig. 3*C*,*D*).

MRS5698 restores the function of proteins involved in the regulation of GABA bioavailability

In experimental neuropathic pain, extracellular GABA is depleted through the downregulation of the GABA-synthesizing enzyme GAD65 and the upregulation of the GABA transporter GAT-1; these biological changes are associated with a reduction in the amount of GABA available to bind to GABA receptors and related pain behaviors. The observed inactivation of GAD65 and activation of GAT-1 are caused by dephosphorylation of their regulatory serine residues (Wei et al., 2004; Cristóvão-Ferreira et al., 2009). We therefore asked whether the development of CCI-induced neuropathic pain is associated with GAD65 and GAT-1 modification and whether those modifications are reversed with MRS5698 treatment. Because previous evidence suggests that changes in both spinal GAD65 and GAT-1 occur ipsilateral to nerve injury (Moore et al., 2002), serine phosphorylation of these proteins was analyzed in dorsal horn tissues ipsilateral to nerve injury and harvested from animals at 1 h after MRS5698 or vehicle administration (peak analgesia) with contralateral tissues within the same animal used as a control. We found that CCI ($n = 10$) decreased the serine phosphorylation of GAD65 (Fig. 4*A*) and GAT-1 (Fig. 4*B*) in immunoprecipitate from ipsilateral dorsal horn as compared to the contralateral side. MRS5698 (1.0 mg/kg; i.p.; $n = 10$) treatment reversed CCI-induced serine dephosphorylation of GAD65 (Fig. 4*A*; Welch's corrected one-tailed two-sample $t_{(14.1)} = -2.2$, $p = 0.021$) and GAT-1 (Fig. 4*B*; Welch's corrected one-tailed two-sample $t_{(12.7)} = -2.3$, $p = 0.021$) consistent with the reestablishment of GABA bioavailability. We observed no changes in total expression levels in either GAD65 (Welch's corrected one-tailed two-sample $t_{(17.9)} = 1.3$, $p = 0.109$) or GAT-1 (Welch's corrected one-tailed two-sample $t_{(15)} = 0.90$, $p = 0.190$).

VU0240551 blocks the anti-allodynic actions of MRS5698

To assess the ability of A_3AR agonists to modulate spinal KCC2, we tested whether spinal KCC2 activity is necessary for MRS5698-mediated reversal of mechano-allodynia. Pretreatment with the selective KCC2 inhibitor, VU0240551 (0.27 μg; i.th.; $n = 6$), abolished the anti-allodynic effects of systemic MRS5698 (1.0 mg/kg; i.p.; $n = 6$). This effect was observed in both the mouse (Fig. 5*A*; repeated-measures ANOVA, $F_{(6,12)} = 25.9$, $p = 0.001$) and rat (Fig. 5*B*; Greenhouse–Geisser corrected repeated-measures ANOVA, $\varepsilon = 0.478$, $F_{(6,12)} = 37$, $p = 0.001$) models of CCI with the dose chosen from previous studies (Delpire et al., 2009; Austin and Delpire, 2011). At the dose tested, VU0240551 did not affect PWT in naive animals (data not shown).

MRS5698 restores KCC2 function in CCI animals

Spinal dorsal horn tissues were collected from CCI rats receiving MRS5698 or vehicle treatment at peak analgesia (1 h after administration) and assayed for phosphoserine and total KCC2 protein expression levels. Similar to GAD65 and GAT-1, previous reports indicated that changes in KCC2 activity and expression only occur ipsilateral to the nerve injury. We found that serine phosphorylation of KCC2 in the ipsilateral dorsal horn was decreased in response to CCI ($n = 10$). MRS5698 administration (1.0 mg/kg; i.p.; $n = 10$) restored serine phosphorylation of KCC2 on the ipsilateral side (Fig. 5*C*; Welch's corrected one-tailed two-sample $t_{(17.7)} = -2.053$, $p = 0.028$). Total KCC2 was not changed in either group (Fig. 5*C*; Welch's corrected one-tailed two-sample $t_{(16.3)} = 0.067$, $p = 0.474$). Phosphorylation of the serine 940 residue on KCC2 is the only site explicitly shown to increase KCC2 activity. Thus, we confirmed that phosphorylation at ser-

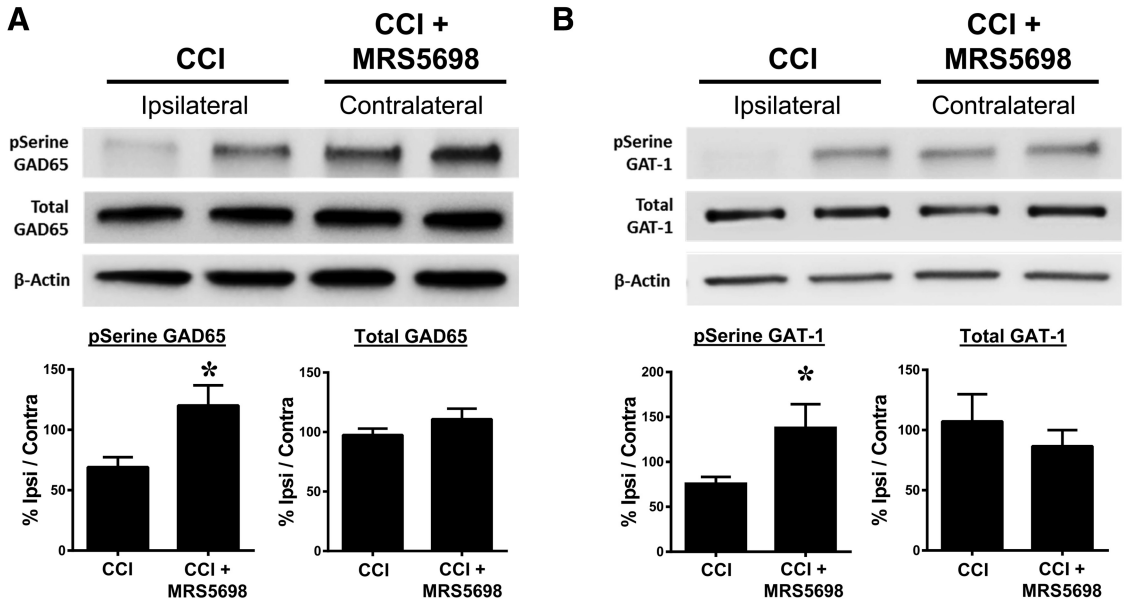

Figure 4. MRS5698 restores GABA availability. In rats with CCI-induced pain treated with vehicle, phosphorylation of serine residues on GAD65 (***A***) and GAT-1 (***B***) was decreased in dorsal horn tissues ipsilateral to the injury when normalized to contralateral control. Treatment with MRS5698 (1.0 mg/kg; i.p.) reversed this CCI-induced dephosphorylation and restored p-serine levels on the ipsilateral side (***A***, ***B***). There were no observed changes in total GAD65 (***A***) or GAT-1 (***B***) expression. Data are mean ± SEM; $n = 10$ rats. *$p < 0.05$ versus Veh (Welch's corrected one-tailed unpaired Student's *t* test).

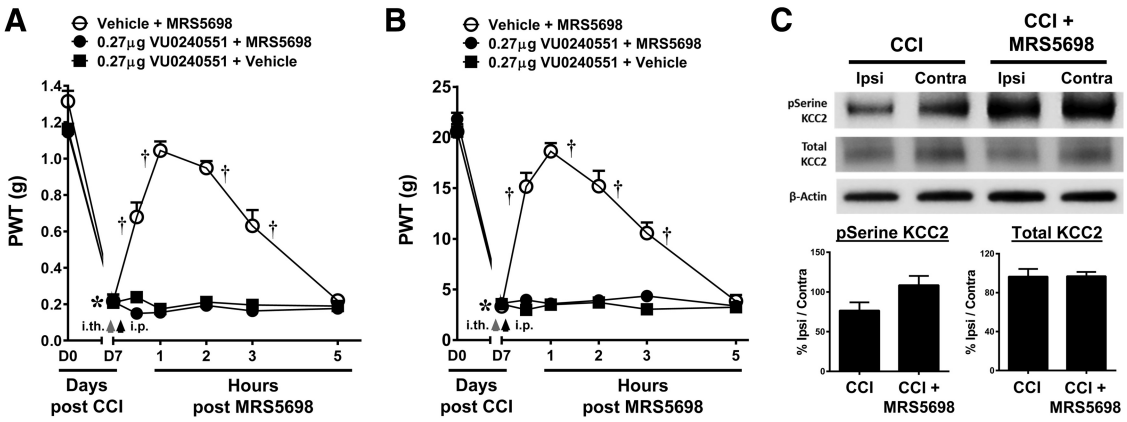

Figure 5. The anti-allodynic actions of MRS5698 involve the restoration of KCC2 activity. In both mouse (***A***) and rat (***B***) models, administration of MRS5698 (black arrow; 1.0 mg/kg; i.p.) led to a time-dependent development of mechano-allodynia, which was blocked by pretreatment with VU0240551 (gray arrow; 0.27 μg; i.th.). VU0240551 alone had no effect. In CCI treated with vehicle, phosphorylation of serine residues on KCC2 was decreased in dorsal horn tissues on the side ipsilateral to the injury compared with contralateral control. Treatment with MRS5698 (1.0 mg/kg; i.p.) reversed these effects and increased pSerine levels on the ipsilateral side (***C***). There were no observed changes in total KCC2 expression in either group (***C***). Data are mean ± SEM; $n = 6$. ***A***, ***B***, Repeated-measures ANOVA with Bonferroni comparisons. ***C***, Welch's corrected one-tailed unpaired Student's *t* test. *$p < 0.05$ for D7 versus D0. †$p < 0.05$ drug versus D7. °$p < 0.05$ CCI + MRS5698 versus CCI.

ine 940 was increased in the ipsilateral spinal cord in CCI animals receiving MRS5698. Indeed, systemic MRS5698 (1.0 mg/kg; i.p.), but not vehicle enhanced pKCC2, in the ipsilateral laminae I and II of the spinal dorsal horn as compared to the contralateral side (Fig. 6*A–C*; Welch's corrected one-tailed two-sample $t_{(6)} = -2.04$, $p = 0.044$).

To assess whether KCC2 serine phosphorylation is associated with changes in KCC2 activity, we assayed the ability of nerve injury to produce a decrease in KCC2-mediated Cl^- transport; furthermore, we asked whether MRS5698 restores normal function of KCC2 in mature neurons. We measured the effect of MRS5698 on Cl^- transport in lamina II of spinal cord slices obtained from rats with CCI and control slices from naive or sham animals. KCC2 function was assessed by measuring K^+-driven Cl^- influx via fluorescence lifetime measurements of the Cl^--sensitive probe MQAE. Changing the $[K^+]_e$ from 2.5 to 15 mM caused inversion of KCC2 transport and subsequent Cl^- accumulation inside cells. The rate of intracellular Cl^- change was measured as an index of KCC2-mediated transport rate. CCI animals displayed a slower rate of Cl^- transport as compared to sham animals (0.069 and −0.117 ns/min, respectively). When treated with MRS5698 (1 mg/kg; $n = 16$; i.p.), the Cl^- transport activity was restored to values obtained from naive rats (−0.109 ns/min in naive animals and −0.109 ns/min in CCI animals treated with MRS5698; Fig. 7*A–C*; one-way ANOVA, $F_{(3)} = 4.2$, $p = 0.013$).

Discussion

Chronic neuropathic pain represents a major public health problem that will only intensify as an aging population suffers from

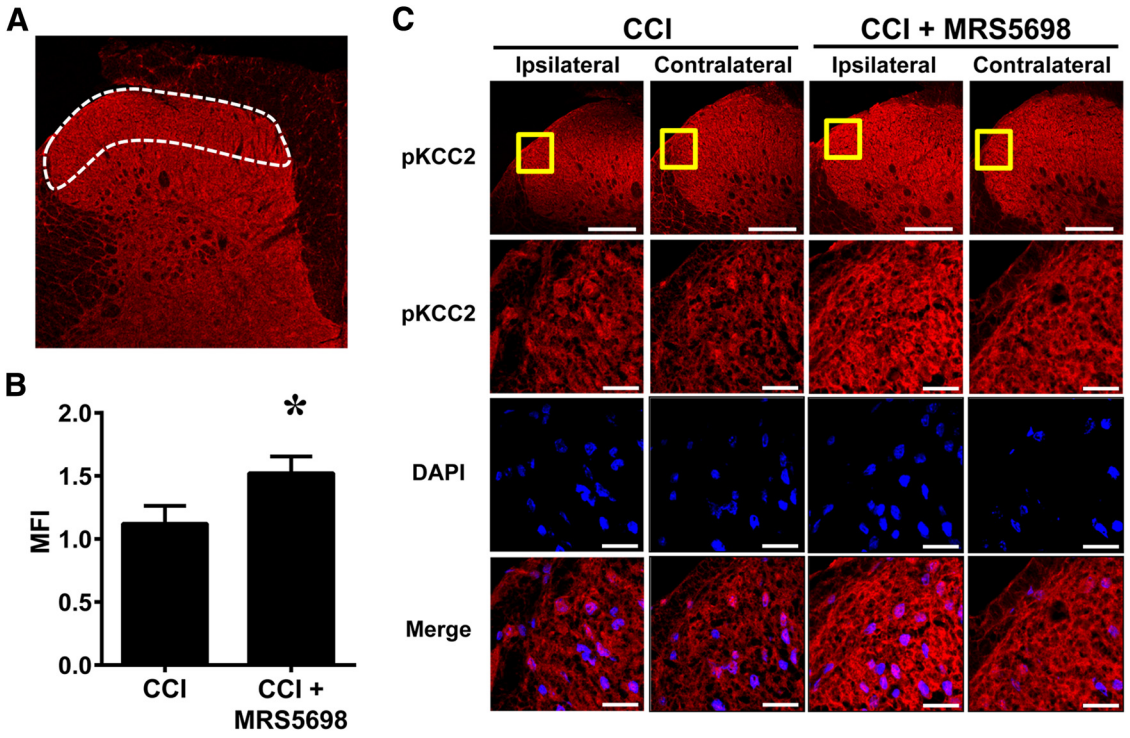

Figure 6. MRS5698 increases phosphorylation of Ser^{940} on KCC2. Compared with contralateral side on D7, MRS5698 (1.0 mg/kg; i.p.), but not vehicle, enhanced pKCC2 immunolabeling (red) in the ipsilateral laminae I and II of the dorsal horn (***A***; white border) (***B***, ***C***). Higher-magnification images (yellow box) of superficial dorsal horn are merged with DAPI (blue) (***C***). Negative controls exhibited low levels of background fluorescence (data not shown). MFI is reported as mean fold change comparing ipsilateral/contralateral. Micrographs represent $n = 4$ rats/group and 3 sections/animal (L4, L5, and L6 spinal cord levels). Data are mean ± SEM in arbitrary units. *$p < 0.05$ versus CCI D7 (Welch's corrected one-tailed unpaired Student's t test). Scale bars: ***A***, 200 μm; ***C***, 20 μm.

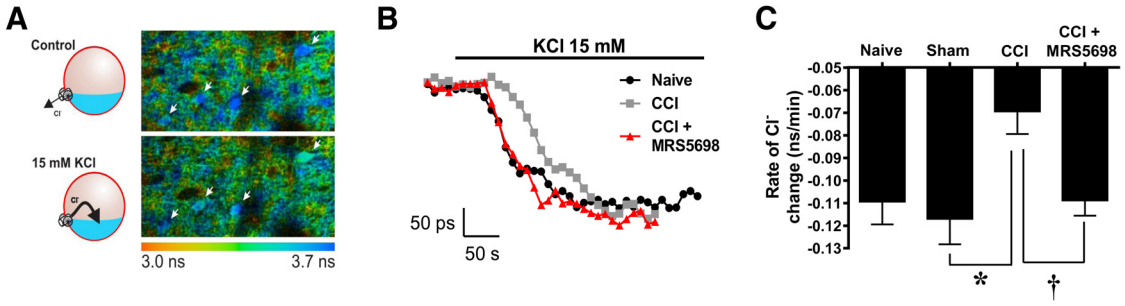

Figure 7. MRS5698 restores KCC2-mediated Cl^- transport. ***A***, Color-coded lifetime image of lamina II cells loaded with the Cl^- indicator MQAE, where lower lifetime values correspond to high Cl^- concentration. A sharp increase of the extracellular [K^+] caused Cl^- accumulation in the cells as measured by the lifetime changes of MQAE. One fluorescence lifetime image was taken every 10 s to follow Cl^- changes through time. The slope of the Cl^- changes is extracted and used as an indication of KCC2 function. In CCI rats ($n = 7$), there is a decrease in KCC2 function. ***B***, Following injection of MRS5698 (1.0 mg/kg; $n = 16$; i.p.), the Cl^- transport rate measured is restored to the level of control and sham values. ***C***, Comparison of the slope of Cl^- changes measured in lamina II cells in sham, CCI animals, and CCI animals treated with MRS5698. Data are mean ± SEM; $n = 6$–16 rats. *$p < 0.05$ for CCI versus sham (one-way ANOVA with Bonferroni's comparisons). †$p <$ 0.05 for CCI + MRS5698 versus CCI (one-way ANOVA with Bonferroni's comparisons).

pain-associated diseases such as arthritis, cancer, and diabetes. Currently, the most effective treatments are either NSAIDs or opiates, which are only moderately effective and exhibit adverse side effects that lead to discontinuation of use (McNicol et al., 2003; Dworkin et al., 2007). Novel mechanism-based treatments for chronic pain are severely lacking and represent a massive unmet clinical need.

Adenosine receptor agonists show potent antinociceptive effects in pain models of various etiologies (Zylka, 2011). However, adenosine-related therapies have been restricted to local delivery as they exhibit dangerous cardiovascular side effects when administered systemically. Recently, we have shown that specific A_3AR agonists have potent analgesic actions in models of chronic neuropathic pain (Chen et al., 2012; Janes et al., 2014, 2015; Little et al., 2015). Given that A_3AR agonists such as IB-MECA are already in Phase II/III clinical trials for psoriasis, hepatitis, rheumatoid arthritis, dry eye, and glaucoma and are exhibiting acceptable safety profiles (Fishman et al., 2012), they show clinical prospective as a novel therapeutic approach to pain.

To examine possible mechanisms underlying the antinociceptive actions of A_3AR agonists, it is important to first understand their pharmacological characteristics and potential sites of action. Here, we confirm and extend our recent finding that A_3AR activation in CNS areas related to pain processing is critical to A_3AR agonist-mediated antinociception (Little et al., 2015). We show that IB-MECA exerts its actions at least in part via a spinal mechanism, as

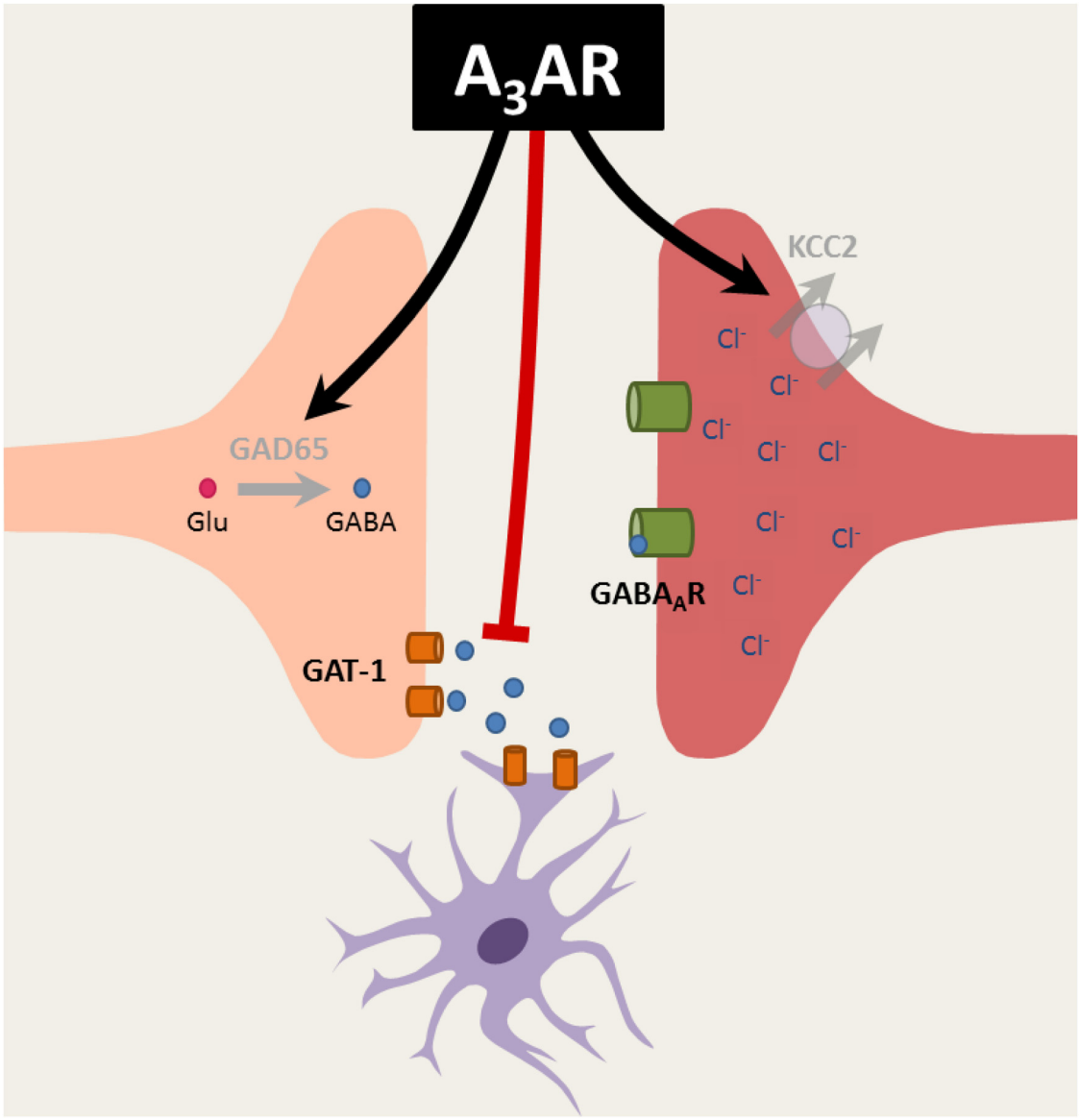

Figure 8. A_3AR agonists modulate key components of the GABAergic signaling pathway. The development of neuropathic pain was associated with dysfunction of GAD65 and GAT-1, both of which can result in less GABA availability within the synapse. Additionally, there was a reduction in the expression and activity of KCC2, which can lead to a buildup of intracellular Cl^- and the blockade of $GABA_A$R-mediated Cl^- influx, resulting in hyperexcitability of the postsynaptic cell. Administration of an A_3AR agonist reversed these nerve injury-induced changes, restoring GAD65 and KCC2 activity while inactivating GAT-1. Therefore, A_3AR agonists may reverse neuropathic pain by enhancing GABA bioavailability within the synaptic cleft while also enhancing its efficacy by potentiating KCC2 activity.

blocking spinal A_3AR activation with MRS1523 precludes the anti-allodynic effects of systemically administered IB-MECA. We corroborate our findings using the chemically distinct and more selective A_3AR agonist MRS5698. Intrathecal administration of MRS5698 dose-dependently reverses mechano-allodynia and spinally administered MRS1523 blocks the antinociception produced by systemically administered MRS5698. Furthermore, we validate our previous findings in a rat CCI model, demonstrating that the proposed A_3AR mechanism is not species-specific and permitting future biochemical analyses that require larger amounts of tissue from a small, specific region of the spinal cord.

The GABAergic signaling pathway plays an integral role in coordinating both the perception of and response to painful stimuli within the CNS; accordingly, GABA dysfunction is implicated in a number of pain states (Enna and McCarson, 2006). Extensive research efforts have been aimed at the development of drugs that enhance GABAergic signaling and have led to the targeting of not only GABA receptors, but also GABA-associated transporters and enzymes (Jasmin et al., 2004) such as GAT-1 (Schousboe et al., 2004) and GAD65 (Jain, 2008; Vit et al., 2009). Consequently, GABA receptor agonists as well as inhibitors of GABA uptake and metabolism display potent antinociceptive properties in a range of preclinical pain models (Enna and McCarson, 2006). Unfortunately, it has proven difficult to exploit GABA-specific strategies as the activation of GABA receptors in non-nociceptive areas of the CNS yields unfavorable side effects. We offer that A_3AR agonists may represent a unique opportunity to tap into the beneficial actions of the GABA signaling pathway while avoiding undesirable side effects in the treatment of chronic pain.

In the present work, we demonstrate that the spinal mechanism of MRS5698 antinociception involves GABA signaling as a

$GABA_A$ antagonist prevents the anti-allodynic action of A_3AR agonists. We did not examine the involvement of the $GABA_B$ receptor subtype as $GABA_A$R mechanisms are more readily investigated and understood in pathological pain states. We show that CCI produces a relative loss of phosphorylation of GAD65, an enzyme responsible for GABA synthesis, and GAT-1, a GABA reuptake transporter, whereas MRS5698 treatment maintains the phosphorylation status of GAD65 and GAT-1. Serine phosphorylation is known to activate GAD65 and stabilize it within the plasma membrane (Wei et al., 2004) and serine phosphorylation of GAT-1 signals for internalization and inactivation of the transporter (Law et al., 2000; Whitworth and Quick, 2001) such that the net effect of MRS5698 treatment is likely to increase synaptic GABA availability. Restriction of the effect of MRS5698 to the ipsilateral (injured) side supports our previous finding that A_3AR plays a prominent role in modulating pathophysiological pain without altering normal protective pain sensation (Chen et al., 2012; Little et al., 2015).

Following peripheral nerve injury, pharmacological enhancements in extracellular GABA can persist beyond the time frame of analgesic efficacy (Cui et al., 1997), suggesting that increases in GABA availability alone fail to compensate for an underlying dysfunction of $GABA_A$Rs in pathological pain. Extensive evidence suggests that this dysfunction is due to the downregulation and decreased activity of KCC2, a postsynaptically restricted Cl^-/K^+ cotransporter that functions to maintain the chloride gradient and is crucial to $GABA_A$-mediated postsynaptic inhibition (Williams et al., 1999; Kahle et al., 2008; Miletic and Miletic, 2008; Janssen et al., 2011). In the present work, we highlight the protective effect of MRS5698 administration on KCC2 function: we demonstrate that the anti-allodynic actions of MRS5698 require KCC2 activity as the selective KCC2 inhibitor, VU0240551, completely abrogates the beneficial effects of MRS5698. Additionally, administration of MRS5698 enhances the serine phosphorylation of KCC2 at Ser940, which is to date the only site explicitly shown to increase KCC2 activity (Lee et al., 2007). Indeed, we demonstrate that the rate of KCC2-dependent Cl^- extrusion is decreased in CCI versus sham animal spinal cord slices, and MRS5698 administration attenuates this loss of Cl^- transport rate. These data indicate that an A_3AR-mediated restoration of KCC2-dependent Cl^- transport in CNS neurons may underlie the ability of MRS5698 to restore GABAergic neurotransmission in neuropathic pain.

To date, it is unknown how A_3AR modifies the phosphorylation status of GAD65, GAT-1, and KCC2 to promote GABA function. One possible mechanism is through the A_3AR-mediated activation of protein kinase C (PKC): CNS A_3ARs can produce PKC activation in neurons by coupling to the G_q intracellular signaling pathway (Abbracchio et al., 1995; Dunwiddie et al., 1997). Previous studies have shown that GAD65 is phosphorylated almost exclusively by PKCε (Wei et al., 2004) and it has been demonstrated that adenosine can activate this PKC isoform in the instance of adenosine-mediated neuroprotection (DiCapua et al., 2003). Furthermore, PKC is responsible for phosphorylating KCC2 on serine, threonine, and tyrosine residues as a mechanism of regulating intrinsic ion transport rate, cell surface stability, and plasmalemmal trafficking (Kahle et al., 2013). Phosphorylation of KCC2 at Ser940 is specifically PKC-dependent (Lee et al., 2007), suggesting that an A_3AR-to-PKC mechanism could feasibly underlie MRS5698-mediated enhancements in GABAergic signaling.

Alternatively, PKC-dependent phosphorylation of spinal KCC2 can be mediated by the serotonin (5-HT) axis: activation of 5-HT_{2A} produces PKC activation of KCC2 in spinal neurons and subsequently strengthened neuronal inhibition (Bos et al., 2013). Although the effect of serotonin in pain can be bidirectional, sufficient evidence implicates activation of 5-HT receptor subtypes in descending nociceptive inhibition: projections from the rostral ventromedial medulla elicit the release of serotonin in the spinal dorsal horn and this action can lead to antinociception (Wei et al., 2010; Hossaini et al., 2012; Ossipov et al., 2014). We have demonstrated the role of A_3AR in descending inhibitory mechanisms (Little et al., 2015); accordingly, the modulation of descending serotonergic projections by MRS5698 could lead to the observed effects on the GABA-to-KCC2 pathway.

In contradistinction, the effects of MRS5698 could be mediated on a broader scale by the neuroinhibitory effects of adenosine on glutamatergic signaling. There is evidence that KCC2 is regulated in an activity-dependent fashion in neurons (Puskarjov et al., 2012) and that this mechanism is relevant in neuropathic pain (Zhou et al., 2012). Indeed, excitatory NMDAR activity can lead to the dephosphorylation of KCC2 at Ser940 (Lee et al., 2011). Because adenosine signaling functions as a vital "fine-tuning" mechanism for neurotransmission in the CNS (Wall and Richardson, 2015) and plays the role of a negative neuromodulator in excitatory synapses (Zhang et al., 2015), A_3AR activation may prevent the activity-dependent dephoshorylation of KCC2 and subsequent dysfunction in GABA signaling.

Lastly, it is important to consider that MRS5698 could elicit changes in GABAergic signaling by abrogating glial-driven mechanisms of GABA dysfunction in neuropathic pain. To this end, glial-derived BDNF signaling is known to play a pronociceptive role in rodent CCI (Chen et al., 2014) by downregulating KCC2 and disrupting Cl^- homeostasis, thereby reducing the strength of $GABA_A$ and glycine receptor-mediated postsynaptic inhibition (Biggs et al., 2010; Ferrini and De Koninck, 2013). In this paper, we have not examined whether the A_3AR impinges upon the BDNF/TrkB/KCC2 pathway and we are not excluding a potential effect of A_3AR agonists on this pathway. It is unlikely that MRS5698 acts directly on TrkB as an off-target because the observations in our manuscript are not consistent with the effects of a TrkB antagonist: in our studies, we have identified Ser940 on KCC2 (Lee et al., 2007) as a critical site of A_3AR-mediated regulation. In contrast, TrkB has only been documented to modify Tyr515 on KCC2 in the CNS (Rivera et al., 2004; Choe et al., 2015), and this phosphorylation event produces transporter internalization rather than an increase in transporter activity. Additionally, TrkB activity is not known to regulate the phosphorylation of GAD65 or GAT-1; it has been suggested that TrkB influences these enzymes through a CREB-dependent mechanism of transcriptional regulation (Sanchez-Huertas and Rico, 2011). On the other hand, it is conceivable that MRS5698 may impact BDNF/TrkB/KCC2 signaling by inhibiting the release of BDNF from glial cells as a parallel mechanism to the phosphorylation events we observe in A_3AR-mediated restoration of GABAergic function. We have previously demonstrated the capacity of A_3AR activation to attenuate astrocyte reactivity and neuroinflammatory response in chemotherapy-induced peripheral neuropathy (Janes et al., 2015) and additionally, A_3AR activation may provide neuroprotection by inhibiting the reactive chemotaxis of microglia (Choi et al., 2011). As such, it is possible that an A_3AR-mediated reduction in glial activation could preclude glial BDNF release and relieve TrkB-mediated alterations in GABA signaling in contribution to the restoration of GABA signaling that we have observed.

Collectively, the findings presented herein provide a pharmacological rationale for the development of A_3AR agonists as a novel approach to the treatment of chronic pain. The present work supports our hypothesis that A_3AR agonists attenuate neuropathic pain through modulation of the GABAergic signaling pathway. These data provide not only important mechanistic data about the action of A_3AR agonists, but also demonstrate the advantage of A_3AR as a two-pronged approach to restoring GABAergic function in chronic pain: enhancing GABA bioavailability within the synaptic cleft while also enhancing its efficacy by potentiating KCC2 activity (summarized in Fig. 8). A_3AR agonists represent a unique opportunity to tap into the potent beneficial actions of two important inhibitory pain pathways (adenosine and GABA) while avoiding the adverse effects observed with modulatory drugs targeted to these pathways to date.

References

Abbracchio MP, Brambilla R, Ceruti S, Kim HO, von Lubitz DK, Jacobson KA, Cattabeni F (1995) G protein-dependant activation of phospholipase C by adenosine A3 receptors in the rat brain. Mol Pharmacol 48:1038–1045. Medline

Austin TM, Delpire E (2011) Inhibition of KCC2 in mouse spinal cord neurons leads to hypersensitivity to thermal stimulation. Anesth Analg 113:1509–1515. CrossRef Medline

Bennett GJ, Xie YK (1988) A peripheral mononeuropathy in rat that produces disorders of pain sensation like those seen in man. Pain 33:87–107. CrossRef Medline

Biggs JE, Lu VB, Stebbing MJ, Balasubramanyan S, Smith PA (2010) Is BDNF sufficient for information transfer between microglia and dorsal horn neurons during the onset of central sensitization? Mol Pain 6:44. CrossRef Medline

Borea PA, Varani K, Vincenzi F, Baraldi PG, Tabrizi MA, Merighi S, Gessi S (2015) The A3 adenosine receptor: history and perspectives. Pharmacol Rev 67:74–102. CrossRef Medline

Bos R, Sadlaoud K, Boulenguez P, Buttigieg D, Liabeuf S, Brocard C, Haase G, Bras H, Vinay L (2013) Activation of 5-HT2A receptors upregulates the function of the neuronal K-Cl cotransporter KCC2. Proc Natl Acad Sci U S A 110:348–353. CrossRef Medline

Chen JT, Guo D, Campanelli D, Frattini F, Mayer F, Zhou L, Kuner R, Heppenstall PA, Knipper M, Hu J (2014) Presynaptic GABAergic inhibition regulated by BDNF contributes to neuropathic pain induction. Nat Commun 5:5331. CrossRef Medline

Chen Z, Janes K, Chen C, Doyle T, Bryant L, Tosh DK, Jacobson KA, Salvemini D (2012) Controlling murine and rat chronic pain through A3 adenosine receptor activation. FASEB J 26:1855–1865. CrossRef Medline

Chéry N, Yu XH, de Koninck Y (2000) Visualization of lamina I of the dorsal horn in live adult rat spinal cord slices. J Neurosci Methods 96:133–142. CrossRef Medline

Choe KY, Han SY, Gaub P, Shell B, Voisin DL, Knapp BA, Barker PA, Brown CH, Cunningham JT, Bourque CW (2015) High salt intake increases blood pressure via BDNF-mediated downregulation of KCC2 and impaired baroflex inhibition of vasopressin neurons. Neuron 85:549–560. CrossRef Medline

Choi IY, Lee JC, Ju C, Hwang S, Cho GS, Lee HW, Choi WJ, Jeong LS, Kim WK (2011) A3 adenosine receptor agonist reduces brain ischemic injury and inhibits inflammatory cell migration in rats. J Pathol 179:2042–2052. CrossRef Medline

Chorin E, Vinograd O, Fleidervish I, Gilad D, Herrmann S, Sekler I, Aizenman E, Hershfinkel M (2011) Upregulation of KCC2 activity by zinc-mediated neurotransmission via the mZnR/GPR39 receptor. J Neurosci 31:12916–12926. CrossRef Medline

Coull JA, Boudreau D, Bachand K, Prescott SA, Nault F, Sík A, De Koninck P, De Koninck Y (2003) Trans-synaptic shift in anion gradient in spinal lamina I neurons as a mechanism of neuropathic pain. Nature 424:938–942. CrossRef Medline

Cristóvão-Ferreira S, Vaz SH, Ribeiro JA, Sebastião AM (2009) Adenosine A2A receptors enhance GABA transport into nerve terminals by restraining PKC inhibition of GAT-1. J Neurochem 109:336–347. CrossRef Medline

Cui JG, O'Connor WT, Ungerstedt U, Linderoth B, Meyerson BA (1997) Spinal cord stimulation attenuates augmented dorsal horn release of excitatory amino acids in mononeuropathy via a GABAergic mechanism. Pain 73:87–95. CrossRef Medline

Daemen MA, Hoogland G, Cijntje JM, Spincemaille GH (2008) Upregulation of the GABA-transporter GAT-1 in the spinal cord contributes to pain behaviour in experimental neuropathy. Neurosci Lett 444:112–115. CrossRef Medline

Delpire E, Days E, Lewis LM, Mi D, Kim K, Lindsley CW, Weaver CD (2009) Small-molecule screen identifies inhibitors of the neuronal K-Cl cotransporter KCC2. Proc Natl Acad Sci U S A 106:5383–5388. CrossRef Medline

Di-Capua N, Sperling O, Zoref-Shani E (2003) Protein kinase C-epsilon is involved in the adenosine-activated signal transduction pathway conferring protection against ischemia-reperfusion injury in primary rat neuronal cultures. J Neurochem 84:409–412. CrossRef Medline

Digman MA, Caiolfa VR, Zamai M, Gratton E (2008) The phasor approach to fluorescence lifetime imaging analysis. Biophys J 94:L14–L16. CrossRef Medline

Dixon WJ (1980) Efficient analysis of experimental observations. Annu Rev Pharmacol Toxicol 20:441–462. CrossRef Medline

Doyle T, Chen Z, Muscoli C, Obeid LM, Salvemini D (2011) Intraplantar-injected ceramide in rats induces hyperalgesia through an NF-kappaB- and p38 kinase-dependent cyclooxygenase 2/prostaglandin E2 pathway. FASEB J 25:2782–2791. CrossRef Medline

Doyon N, Prescott SA, Castonguay A, Godin AG, Kröger H, De Koninck Y (2011) Efficacy of synaptic inhibition depends on multiple, dynamically interacting mechanisms implicated in chloride homeostasis. PLoS Comput Biol 7:e1002149. CrossRef Medline

Dunwiddie TV, Diao L, Kim HO, Jiang JL, Jacobson KA (1997) Activation of hippocampal adenosine A3 receptors produces a desensitization of A1 receptor-mediated responses in rat hippocampus. J Neurosci 17:607–614. Medline

Dworkin RH, O'Connor AB, Backonja M, Farrar JT, Finnerup NB, Jensen TS, Kalso EA, Loeser JD, Miaskowski C, Nurmikko TJ, Portenoy RK, Rice AS, Stacey BR, Treede RD, Turk DC, Wallace MS (2007) Pharmacologic management of neuropathic pain: evidence-based recommendations. Pain 132:237–251. CrossRef Medline

Eaton MJ, Plunkett JA, Karmally S, Martinez MA, Montanez K (1998) Changes in GAD- and GABA-immunoreactivity in the spinal dorsal horn after peripheral nerve injury and promotion of recovery by lumbar transplant of immortalized serotonergic precursors. J Chem Neuroanat 16:57–72. CrossRef Medline

Enna SJ, McCarson KE (2006) The role of GABA in the mediation and perception of pain. Adv Pharmacol 54:1–27. CrossRef Medline

Ferrini F, De Koninck Y (2013) Microglia control neuronal network excitability via BDNF signalling. Neural Plasticity 2013:429815. CrossRef Medline

Ferrini F, Trang T, Mattioli TA, Laffray S, Del'Guidice T, Lorenzo LE, Castonguay A, Doyon N, Zhang W, Godin AG, Mohr D, Beggs S, Vandal K, Beaulieu JM, Cahill CM, Salter MW, De Koninck Y (2013) Morphine hyperalgesia gated through microglia-mediated disruption of neuronal Cl(−) homeostasis. Nat Neurosci 16:183–192. CrossRef Medline

Fishman P, Bar-Yehuda S, Liang BT, Jacobson KA (2012) Pharmacological and therapeutic effects of A3 adenosine receptor agonists. Drug Discov Today 17:359–366. CrossRef Medline

Hossaini M, Goos JA, Kohli SK, Holstege JC (2012) Distribution of glycine/GABA neurons in the ventromedial medulla with descending spinal projections and evidence for an ascending glycine/GABA projection. PLoS One 7:e35293. CrossRef Medline

Jain KK (2008) Gene therapy for pain. Expert Opin Biol Ther 8:1855–1866. CrossRef Medline

Janes K, Esposito E, Doyle T, Cuzzocrea S, Tosh DK, Jacobson KA, Salvemini D (2014) A3 adenosine receptor agonist prevents the development of paclitaxel-induced neuropathic pain by modulating spinal glial-restricted redox-dependent signaling pathways. Pain 155:2560–2567. CrossRef Medline

Janes K, Wahlman C, Little JW, Doyle T, Tosh DK, Jacobson KA, Salvemini D (2015) Spinal neuroimmune activation is independent of T-cell infiltration and attenuated by A3 adenosine receptor agonists in a model of oxaliplatin-induced peripheral neuropathy. Brain Behav Immun 44:91–99. CrossRef Medline

Janssen SP, Truin M, Van Kleef M, Joosten EA (2011) Differential GABAe-

rgic disinhibition during the development of painful peripheral neuropathy. Neuroscience 184:183–194. CrossRef Medline

Jasmin L, Wu MV, Ohara PT (2004) GABA puts a stop to pain. Curr Drug Targets CNS Neurol Disord 3:487–505. CrossRef Medline

Kahle KT, Staley KJ, Nahed BV, Gamba G, Hebert SC, Lifton RP, Mount DB (2008) Roles of the cation-chloride cotransporters in neurological disease. Nat Clin Pract Neurol 4:490–503. CrossRef Medline

Kahle KT, Deeb TZ, Puskarjov M, Silayeva L, Liang B, Kaila K, Moss SJ (2013) Modulation of neuronal activity by phosphorylation of the K-Cl cotransporter KCC2. Trends Neurosci 36:726–737. CrossRef Medline

Law RM, Stafford A, Quick MW (2000) Functional regulation of gamma-aminobutyric acid transporters by direct tyrosine phosphorylation. J Biol Chem 275:23986–23991. CrossRef Medline

Lee HH, Walker JA, Williams JR, Goodier RJ, Payne JA, Moss SJ (2007) Direct protein kinase C-dependent phosphorylation regulates the cell surface stability and activity of the potassium chloride cotransporter KCC2. J Biol Chem 282:29777–29784. CrossRef Medline

Lee HH, Deeb TZ, Walker JA, Davies PA, Moss SJ (2011) NMDA receptor activity downregulates KCC2 resulting in depolarizing GABAA receptor-mediated currents. Nat Neurosci 14:736–743. CrossRef Medline

Li AH, Moro S, Melman N, Ji XD, Jacobson KA (1998) Structure-activity relationships and molecular modeling of 3, 5-diacyl-2,4-dialkylpyridine derivatives as selective A3 adenosine receptor antagonists. J Med Chem 41:3186–3201. CrossRef Medline

Little JW, Chen Z, Doyle T, Porreca F, Ghaffari M, Bryant L, Neumann WL, Salvemini D (2012) Supraspinal peroxynitrite modulates pain signaling by suppressing the endogenous opioid pathway. J Neurosci 32:10797–10808. CrossRef Medline

Little JW, Ford A, Symons-Liguori AM, Chen Z, Janes K, Doyle T, Xie J, Luongo L, Tosh DK, Maione S, Bannister K, Dickenson AH, Vanderah TW, Porreca F, Jacobson KA, Salvemini D (2015) Endogenous adenosine A3 receptor activation selectively alleviates persistent pain states. Brain 138:28–35. CrossRef Medline

Liu C, Guo QL, Huang CS, Zou WY, Song ZB (2013) Suppressing SNAP-25 and reversing glial glutamate transporters relieves neuropathic pain in rats by ameliorating imbalanced neurotransmission. Chin Med J (Engl) 126:4100–4104. Medline

Malan TP, Mata HP, Porreca F (2002) Spinal GABA(A) and GABA(B) receptor pharmacology in a rat model of neuropathic pain. Anesthesiology 96:1161–1167. CrossRef Medline

McCarson KE, Enna SJ (2014) GABA pharmacology: the search for analgesics. Neurochem Res 39:1948–1963. CrossRef Medline

McNicol E, Horowicz-Mehler N, Fisk RA, Bennett K, Gialeli-Goudas M, Chew PW, Lau J, Carr D (2003) Management of opioid side effects in cancer-related and chronic noncancer pain: a systematic review. J Pain 4:231–256. CrossRef Medline

Miletic G, Miletic V (2008) Loose ligation of the sciatic nerve is associated with TrkB receptor-dependent decreases in KCC2 protein levels in the ipsilateral spinal dorsal horn. Pain 137:532–539. CrossRef Medline

Moore KA, Kohno T, Karchewski LA, Scholz J, Baba H, Woolf CJ (2002) Partial peripheral nerve injury promotes a selective loss of GABAergic inhibition in the superficial dorsal horn of the spinal cord. J Neurosci 22:6724–6731. Medline

Nowak LM, Young AB, Macdonald RL (1982) GABA and bicuculline actions on mouse spinal cord and cortical neurons in cell culture. Brain Res 244:155–164. CrossRef Medline

Ossipov MH, Morimura K, Porreca F (2014) Descending pain modulation and chronification of pain. Curr Opin Support Palliat Care 8:143–151. CrossRef Medline

Paoletta S, Tosh DK, Salvemini D, Jacobson KA (2014) Structural probing of off-target G protein-coupled receptor activities within a series of adenosine/adenine congeners. PLoS One 9:e97858. CrossRef Medline

Paxinos G, Watson C (1998) The rat brain in stereotaxic coordinates, Ed 4. San Diego: Academic.

Price TJ, Cervero F, de Koninck Y (2005) Role of cation-chloride-cotransporters (CCC) in pain and hyperalgesia. Curr Top Med Chem 5:547–555. CrossRef Medline

Puskarjov M, Ahmad F, Kaila K, Blaesse P (2012) Activity-dependent cleavage of the K-Cl cotransporter KCC2 mediated by calcium-activated protease calpain. J Neurosci 32:11356–11364. CrossRef Medline

Rasband WS (1997–2011) ImageJ. Bethesda, MD: National Institutes of Health.

Rivera C, Voipio J, Kalia K (2004) Two developmental switches in GABAergic signaling: the K^+-Cl^- contransporter KCC3 and carbonic anhydrase CAVII. J Physiol 562:27–36. CrossRef Medline

Salvatore CA, Jacobson MA, Taylor HE, Linden J, Johnson RG (1993) Molecular cloning and characterization of the human A3 adenosine receptor. Proc Natl Acad Sci U S A 90:10365–10369. CrossRef Medline

Samways DS, Khakh BS, Dutertre S, Egan TM (2011) Preferential use of unobstructed lateral portals as the access route to the pore of human ATP-gated ion channels (P2X receptors). Proc Natl Acad Sci U S A 108:13800–13805. CrossRef Medline

Sanchez-Huertas C, Rico B (2011) CREB-dependent regulation of GAD65 transcription by BDNF/TrkB in cortical interneurons. Cereb Cortex 21:777–788. CrossRef Medline

Sawynok J (2007) Adenosine and ATP receptors. Handb Exp Pharmacol 177:309–328. Medline

Schousboe A, Sarup A, Larsson OM, White HS (2004) GABA transporters as drug targets for modulation of GABAergic activity. Biochem Pharmacol 68:1557–1563. CrossRef Medline

Stiller CO, Cui JG, O'Connor WT, Brodin E, Meyerson BA, Linderoth B (1996) Release of gamma-aminobutyric acid in the dorsal horn and suppression of tactile allodynia by spinal cord stimulation in mononeuropathic rats. Neurosurgery 39:367- 374, discussion 374–375. CrossRef Medline

Tosh DK, Deflorian F, Phan K, Gao ZG, Wan TC, Gizewski E, Auchampach JA, Jacobson KA (2012) Structure-guided design of A(3) adenosine receptor-selective nucleosides: combination of 2-arylethynyl and bicyclo[3.1.0]hexane substitutions. J Med Chem 55:4847–4860. CrossRef Medline

Vit JP, Ohara PT, Sundberg C, Rubi B, Maechler P, Liu C, Puntel M, Lowenstein P, Castro M, Jasmin L (2009) Adenovector GAD65 gene delivery into the rat trigeminal ganglion produces orofacial analgesia. Mol Pain 5:42. CrossRef Medline

Wall MJ, Richardson MJ (2015) Localised adenosine signalling provides fine-tuned negative feedback over a wide dynamic range of neocortical network activities. J Neurophysiol 113:871–882. CrossRef Medline

Wei F, Dubner R, Zou S, Ren K, Bai G, Wei D, Guo W (2010) Molecular depletion of descending serotonin unmasks its novel facilitatory role in the development of persistent pain. J Neurosci 30:8624–8636. CrossRef Medline

Wei J, Davis KM, Wu H, Wu JY (2004) Protein phosphorylation of human brain glutamic acid decarboxylase (GAD)65 and GAD67 and its physiological implications. Biochemistry 43:6182–6189. CrossRef Medline

Whitworth TL, Quick MW (2001) Substrate-induced regulation of gamma-aminobutyric acid transporter trafficking requires tyrosine phosphorylation. J Biol Chem 276:42932–42937. CrossRef Medline

Williams JR, Sharp JW, Kumari VG, Wilson M, Payne JA (1999) The neuron-specific K-Cl cotransporter, KCC2: antibody development and initial characterization of the protein. J Biol Chem 274:12656–12664. CrossRef Medline

Zeilhofer HU, Wildner H, Yévenes GE (2012) Fast synaptic inhibition in spinal sensory processing and pain control. Physiol Rev 92:193–235. CrossRef Medline

Zhang P, Bannon NM, Ilin V, Volgushev M, Chistiakova M (2015) Adenosine effects on inhibitory synaptic transmission and excitation-inhibition balance in the rat neocortex. J Physiol 593:825–841. CrossRef Medline

Zhou HY, Chen SR, Byun HS, Chen H, Li L, Han HD, Lopez-Berestein G, Sood AK, Pan HL (2012) *N*-Methyl-D-aspartate receptor- and calpain-mediated proteolytic cleavage of K+-Cl^- cotransporter-2 impairs spinal chloride homeostasis in neuropathic pain. J Biol Chem 287:33853–33864. CrossRef Medline

Zylka MJ (2011) Pain-relieving prospects for adenosine receptors and ectonucleotidases. Trends Mol Med 17:188–196. CrossRef Medline